Video Quality Provisioning for Millimeter Wave 5G Cellular Networks With Link Outage

Jian Qiao, Xuemin (Sherman) Shen, *Fellow, IEEE*, Jon W. Mark, *Life Fellow, IEEE*, and Lei Lei

***Abstract*—Millimeter wave (mmWave) communication is a promising solution for future fifth generation (5G) cellular networks to offer extremely high capacity. Because of the propagation characteristics of mmWave band, 5G users with high mobility in metropolitan areas could suffer frequent link outages resulting in challenges on video quality provisioning. In this paper, a playout buffer is used to regulate and maintain the video playout quality. We formulate the problem of using dynamically allocated bandwidth to charge the buffer as a Markov decision process (MDP), aiming to maximize video playout quality for all the users moving in the whole coverage area. Dynamic programming is adopted to solve the MDP problem with state aggregation considering the characteristics of mmWave network. Numerical results demonstrate that the resultant optimal policy of the MDP model can effectively maintain video playout quality for high-mobility users with intermittent mmWave connection.**

***Index Terms*—Millimeter wave, 5G cellular networks, link outage, video quality provisioning.**

I. Introduction

FUTURE 5G cellular networks come with fundamental changes to satisfy the overwhelming capacity demands, brought on by the continuing advances and discoveries in computing and communications [1]–[4]. 5G cellular networks are expected to provide data rates of multi-Gbps range for bandwidth-intensive multimedia applications with stringent quality of service (QoS) requirements (e.g., uncompressed video streaming requires mandatory rate of 1.78 or 3.56 Gbps). To achieve this, more spectrum availability is essential. Millimeter wave (mmWave) communication is a very promising solution for future 5G cellular networks to overcome the global bandwidth shortage at saturated microwave spectrum for most commercial access technologies [1].

mmWave communication has huge available bandwidth [2], which can be translated directly into extremely high capacity [5], [6]. The recent advances of mmWave Radio Frequency Integrated Circuits (RFIC) design also motivate the intensive industrial interest in leveraging mmWave communication for future 5G cellular networks [7]. However, a few challenges on network connectivity could be created by the unique propagation characteristics of mmWave band. First, the mmWave band has limited diffraction capability because of the short wavelength. The line-of-sight (LOS) transmissions can be easily blocked by obstacles and moving people. Since non-line-of-sight (NLOS) transmissions suffer from significant attenuation and a shortage of multipaths [8], link outage can happen if LOS link is blocked. Second, mmWave signals have difficulties in penetrating through solid building materials, e.g., at 40 GHz, 178 dB attenuation for brick wall [2], [9]. Such high attenuation makes mmWave connection unavailable sometimes in an environment with dense high-rise buildings. mmWave link outage can occur more frequently in such environment for high-mobility users, such as vehicular users.

The fundamental question is how to maintain the video playout quality for high-mobility 5G users suffering from frequent mmWave link outage. We embed a buffer in each mobile device to store the data transmitted with extra allocated mmWave bandwidth when mobile user is in the areas with mmWave connection available. Larger allocated mmWave bandwidth can result in more data stored in the buffer, and thus the mobile users can maintain video playout quality for a specific time duration even if they move into areas where mmWave connection is unavailable. On the other hand, with larger allocated mmWave bandwidth to each user, fewer users can be supported in the network, causing inefficient resource utilization. Additionally, due to finite buffer size, larger allocated bandwidth can result in packet overflow and quality loss for video applications. Therefore, how to properly allocate the mmWave bandwidth to dynamically charge or discharge the buffer to maintain the playout quality of multimedia applications is an important and challenging issue.

There are three main contributions in this paper to deal with the challenges mentioned above for video quality provisioning in mmWave 5G cellular networks. First, a buffer system to store the data used for the period when mmWave connection is unavailable is proposed to maintain the playout quality. Second, we formulate the dynamic bandwidth allocation problem in mmWave network as a Markov decision process to maximize the playout quality for a number of moving users with finite buffer size in the coverage area. Third, to provide a general and applicable solution to the Markov decision process, we propose an approximate dynamic programming solution with state aggregation considering the characteristics of the mmWave network.

The remainder of the paper is organized as follows. In Section II, related works are presented. Network architecture and the proposed buffer system are described in Section III. In

Manuscript received November 17, 2014; revised March 17, 2015 and May 19, 2015; accepted May 19, 2015. Date of publication June 4, 2015; date of current version October 8, 2015. The associate editor coordinating the review of this paper and approving it for publication was D. Niyato.

J. Qiao, X. Shen, and J. W. Mark are with the Department of Electrical and Computer Engineering, University of Waterloo, Waterloo, ON N2L 3G1, Canada (e-mail: jqiao@bbcr.uwaterloo.ca; xshen@bbcr.uwaterloo.ca; jwmark@bbcr.uwaterloo.ca).

L. Lei is with the State Key Laboratory of Rail Traffic Control and Safety, Beijing Jiaotong University, Beijing 100044, China (e-mail: leil@bjtu.edu.cn).

Color versions of one or more of the figures in this paper are available online at http://ieeexplore.ieee.org.

Digital Object Identifier 10.1109/TWC.2015.2441708

Section IV, the Markov decision process model is given. An approximate solution is proposed in Section V. Numerical results are shown in Section VI, followed by concluding remarks in Section VII.

II. Related Work

Quality provisioning in wireless networks has been intensively studied in [10]–[19]. One category of video quality provisioning research focuses on wireless resource allocation [10]–[16]. Load-balancing between cellular networks and wireless local area networks (WLANs) considers the available networks individually to satisfy the bandwidth requirements of video application [10]–[12]. In [10], an economic model is used to allocate radio resource between 3G cellular network and WLAN network, aiming to optimize the total welfare of the two networks. In [11], the performance of WLAN-first admission scheme is analyzed for cellular and WLAN integrated networks. In [12], a generalized admission control scheme is considered to analyze the dependence of resource utilization and the impact of user mobility and traffic characteristics on admission parameters. To fully exploit the available resources of multiple networks, quality provisioning in [13]–[15] assumes that each mobile station can jointly utilize the available resources from multiple networks. In [13], video applications attain the bandwidth from 4G cellular network and WLAN to maximize the system utility based on the load characteristics of each network. Literature [14] provides a practical resource allocation scheme in a distributed manner for 3G mobile users with multihoming capability, considering both constant bit rate (CBR) and variable bit rate (VBR) traffic. Most of these works focus on how to allocate the resources to achieve video quality provisioning without addressing mmWave link outage problem which does not occur frequently in microwave frequency band.

Another category of video quality provisioning is to mitigate the effect of wireless channel fluctuation by buffering a certain amount of video data to reduce video playout freezing [17]–[19]. In [17], an analytical framework is developed to investigate the impacts of network dynamics on the user perceived video quality by modeling the playback buffer at the receiver by a G/G/1/M and G/G/1/N queue. To reduce the video frozenness possibility resulting from buffer starvation during the playback period, mobile video applications (e.g., Youtube) tend to download video data aggressively in a periodical manner without the consideration of buffer status and network bandwidth availability [18]. In [19], an intelligent cost-aware buffer management strategy for mobile video streaming applications is proposed to minimize cost induced by un-consumed video data while respecting certain user experience requirements.

Video quality provisioning is a significant issue in mmWave networks due to the intermittent connection. mmWave link outage problem has been investigated in mmWave WLANs/WPANs [20], [21]. A hop selection metric is proposed to select appropriate relay hops to replace the blocked link and improve flow throughput [20]. A multi-hop concurrent transmission scheduling scheme is then proposed to allow multiple hops to operate simultaneously in order to improve system capacity. In [21], cross-layer modeling and design approaches are used to address the problem of directionality and link blockage due to the limited ability to diffract around obstacles. It uses minimum number of hops for data transmission. The relaying method is not suitable to solve mmWave link outage problem in 5G cellular networks since it involves long setup time with directional communication to discover the blocked link, select the relays, and re-build the path. Users with high mobility suffer from very frequent link outage and the relaying method should be repeated very frequently, resulting in significant video quality degradation.

In this paper, we jointly consider the bandwidth allocation and buffer management to provide video quality provisioning for 5G mobile users in order to overcome the impact of mmWave link outage. Compared with existing work on buffer management, the novelty of this paper includes: 1) due to user mobility, limited penetration and diffraction capability, mmWave connection would suffer from frequent link outage which makes buffer management more difficult than that at lower frequency band with channel fluctuation; 2) most of the existing works consider buffer management to provide video quality provisioning for a single user. This paper optimizes the video playout quality for all the users in the system over long time period under the capacity constraint of each mmWave base station considering the movement of each user; and 3) the allocated bandwidth for users in each stage can achieve optimality on video playout quality, i.e., allocating proper bandwidth in each stage, rather than heuristic bandwidth allocation scheme or bandwidth allocation without consideration of buffer status and connection availability.

III. System Model

In this section, the system model is described, including the heterogeneous network architecture with embedded buffer to maintain playout quality for multimedia applications, and the coverage model based on mmWave signal propagation.

A. Heterogeneous Architecture With Embedded Buffer

Current 4G cellular network operating in microwave frequency band can provide seamless coverage and reliable communication. To achieve smooth and cost-efficient transition from 4G to 5G, the hybrid 4G+mmWave system structure shown in Fig. 1 is a good candidate for 5G to provide ubiquitous coverage and high data rate in most coverage areas. 5G cellular networks are expected to support multiple kinds of applications. Low rate applications (such as voice call and Web browsing) can be supported with perfect QoS in 4G network. In this paper, we consider the challenging case, playout quality provisioning for non-real time multimedia applications with high CBR requirement (such as video streaming) in mmWave network.

The hybrid system is composed of 4G base stations, mmWave base stations, and mobile stations. 4G based stations are deployed in the center of each cell while mmWave base stations are deployed densely in small cells with grid topology to provide high data rates and aggregate capacity. Each mobile station has both mmWave access mode and 4G access mode, with fast mode transition between them. All mobile stations and

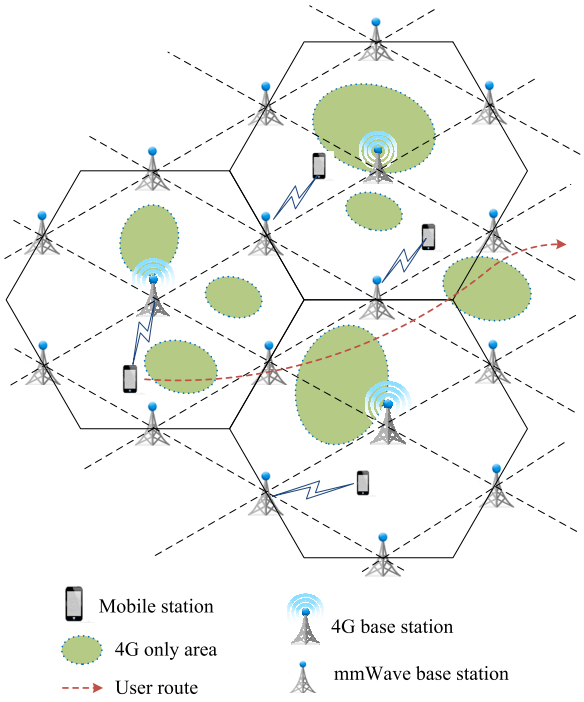

Fig. 1. 5G heterogeneous system architecture with mmWave coverage holes.

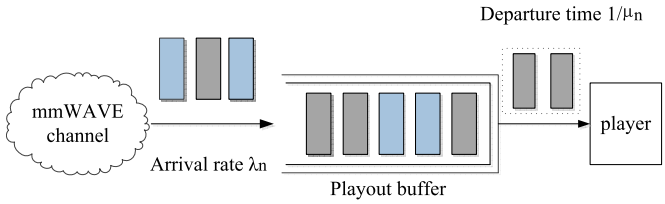

Fig. 2. Buffer system to maintain QoS at end user.

4G base stations have omni-directional antenna for 4G communications. All mobile stations and mmWave base stations are equipped with electronically steerable directional antennas with beamforming technologies [22] for mmWave communication.

As discussed in Section I, frequent link outage could occur to mmWave signal because of the limited diffraction and penetration capability. mmWave transmission rate could descend dramatically with link outage, which results in video frozenness. To improve user's video playout quality, we propose an integrated system with playout buffer to deal with mmWave link outage problem. As shown in Fig. 2, the data is transmitted through mmWave channel to the buffer. The data in the buffer is combined into frames and injected into the end user. Video playout quality can be maintained for a specific period after mmWave link outage occurs, with the data stored in the buffer. Mobile users alternatively move between areas with mmWave connection and areas without mmWave connection, and the playout buffer can be charged or discharged dynamically.

B. mmWave Propagation and Coverage

Slow fading is considered in mmWave propagation. Instantaneous path loss values in dB of mmWave signal are generated using statistical model [23], [24]

TABLE I
PROPAGATION PARAMETERS

LOS	Θ_{LOS}=32.5	ϕ_{LOS}=2.0	σ_{LOS}=0
NLOS	Θ_{NLOS}=44.7	ϕ_{NLOS}=1.5	σ_{NLOS}=3.3

$$PL(d)[dB] = \Theta + 20log_{10}(f) + 10\phi log_{10}(d) + \mathbb{E} \quad (1)$$

where ϕ is the path loss exponent; Θ is the parameter specified for scenario and antenna configuration; and $\mathbb{E}$ is a random variable which describes shadow fading effect with $\mathbb{E} = 0$ for LOS scenario. For outdoor scenario, because of the directional antenna and high frequency band, mmWave propagation is short of reflections and multi-paths. Thus, only LOS transmissions are considered in mmWave outdoor communication [25]. For indoor environments [23], $\mathbb{E}$ follows Gaussian distribution in dB (log-normal distribution in absolute scale) with zero mean and shadow fading standard deviation σ for NLOS scenario. The path loss parameters for LOS scenario and indoor NLOS scenario are shown in Table I [29].

With the above path loss model, the whole area in Fig. 1 can be classified into two categories (namely single-coverage areas and double-coverage areas) based on the instantaneous path loss. The areas satisfying

$$PL(d)[dB] \geq PL_{thr} \quad (2)$$

are considered as single-coverage areas, where PL_{thr} is the path loss threshold to determine if the mmWave connection is available. Other areas with $PL(d)[dB] < PL_{thr}$ are defined as double-coverage areas. As shown in Fig. 1, there are some single-coverage areas without mmWave connection disjointedly distributed in whole area. Mobile users pass through the single-coverage and double-coverage areas alternatively.

IV. PROBLEM FORMULATION

In this section, the problem of bandwidth allocation and video playout quality provisioning for $\mathcal{N}$ mobile users dynamically moving in the whole coverage area is formulated as an MDP problem composed of *the state space*, *the control space*, *the state transition probabilities* and *the cost function*.

A two-dimensional 5G system with a set of M mmWave base stations ($B = \{B_1, B_2, \ldots B_M\}$) is considered in this paper. Each mmWave base station B_m has a specific capacity C_m with $C_m \in \mathfrak{C} = \{C_1, C_2, \ldots C_M\}$. The capacity C_m can be affected by several factors, such as transmission range and building distributions in the cell. It is assumed that the capacity set $\mathfrak{C}$ is available for a given 5G system. The mth cell covered by base station B_m is partitioned into S_m regions. The total number of regions is $S = \sum_{m=1}^{M} S_m$ and we denote each region as $\boldsymbol{s} \in \mathcal{S} = \{1, 2, 3, \ldots, S\}$. Each region $\boldsymbol{s}$ is small enough so that the propagation effects on all signals in region $\boldsymbol{s}$ can be considered to be equivalent. Therefore, the users in each region $\boldsymbol{s}$ can be assumed to have the same instantaneous transmission rate. With AWGN channel, the instantaneous transmission data rate (denoted as $R_{\boldsymbol{s}}$) for all users in each region $\boldsymbol{s}$ can be estimated

by Shannon capacity formula. Since mmWave network adopts TDMA/STDMA-based MAC [20], [26], [27] (i.e., the users associated with each mmWave base station share the mmWave channel by obtaining a specific number of time slots among all the time slots within each superframe), the allocated bandwidth to the nth mobile user U_n in region $\boldsymbol{s}$ can be a portion of the instantaneous rate $R_{\boldsymbol{s}}$. Given a set of available rates in each region $\mathbb{R}_{\boldsymbol{s}} = \left\{0, \frac{1}{\mathcal{K}}R_{\boldsymbol{s}}, \frac{2}{\mathcal{K}}R_{\boldsymbol{s}}, \ldots, R_{\boldsymbol{s}}\right\}$, the allocated bandwidth to the nth mobile user U_n in region $\boldsymbol{s}$ denoted by $B_{n,\boldsymbol{s}}$ could be $B_{n,\boldsymbol{s}} = \frac{k}{\mathcal{K}}R_{\boldsymbol{s}}$ with $k = 0, 1, 2, \ldots, \mathcal{K}$, where k is the number of time slots allocated to mobile user U_n and $\mathcal{K}$ is the total number of time slots in each frame. To make the analysis tractable, $R_{\boldsymbol{s}} = 0$ if region $\boldsymbol{s}$ is single-coverage area.

A. The State Space

Given the set of regions in the whole area $\mathcal{S} = \{1, 2, 3, \ldots, \boldsymbol{s}, \ldots, S\}$ and the set of active users $\mathcal{U} = \{U_1, U_2, \ldots, U_n, \ldots U_{\mathcal{N}}\}$, bandwidth allocation in 5G system at any particular time is then characterized by a $\mathcal{N} \times S$ matrix:

$$\mathbb{B} = \|B_{n,\boldsymbol{s}}\|_{\mathcal{N}\times S} = \begin{Vmatrix} B_{1,1} & B_{1,2} & \cdots & B_{1,S} \\ B_{2,1} & B_{2,2} & \cdots & B_{2,S} \\ \vdots & \vdots & \ddots & \vdots \\ B_{\mathcal{N},1} & B_{\mathcal{N},2} & \cdots & B_{\mathcal{N},S} \end{Vmatrix} \tag{3}$$

where $B_{n,\boldsymbol{s}}$ is the allocated bandwidth to user U_n in region $\boldsymbol{s}$ and is defined as

$$B_{n,\boldsymbol{s}} = \begin{cases} \frac{k}{\mathcal{K}}R_s, & (U_n \text{ in } \boldsymbol{s}) \\ 0, & (\text{otherwise}) \end{cases} \tag{4}$$

$B_{n,\boldsymbol{s}} = 0$ occurs either user U_n is not in region $\boldsymbol{s}$ or mmWave connection is unavailable in region $\boldsymbol{s}$ even if user U_n is located in region $\boldsymbol{s}$. Since each user U_n can only locate in one specific region at any particular time, at most one element in each row of matrix $\mathbb{B}$ is non-zero.

To describe the random movement of the users $\mathcal{U} = \{U_1, U_2, \ldots, U_n, \ldots U_{\mathcal{N}}\}$ among the regions $\mathcal{S} = \{1, 2, 3, \ldots, \boldsymbol{s}, \ldots, S\}$, the following $\mathcal{N} \times S$ matrix is defined,

$$\mathbb{W} = \|w_{n,\boldsymbol{s}}\|_{\mathcal{N}\times S} = \begin{Vmatrix} w_{1,1} & \cdots & w_{1,S} \\ \vdots & \ddots & \vdots \\ w_{\mathcal{N},1} & \cdots & w_{\mathcal{N},S} \end{Vmatrix} \tag{5}$$

where

$$w_{n,\boldsymbol{s}} = \begin{cases} -1, & (U_n \text{ moves out of } \boldsymbol{s}) \\ 1, & (U_n \text{ moves into } \boldsymbol{s}) \\ 0, & (\text{otherwise}). \end{cases} \tag{6}$$

Given a user U_n moving from region $\boldsymbol{s}$ to $\boldsymbol{s}'$, we have $w_{n,\boldsymbol{s}} = -1$ and $w_{n,\boldsymbol{s}'} = 1$. The process of all the users moving in the whole coverage area is very complex. To make the process tractable, it is assumed that the process of all the users moving among different regions is composed of a series of random events, each of which describes a single user movement characterized by the matrix $\mathbb{W}$. Thus, there are only two elements with non-zero value in the matrix $\mathbb{W}$ and all the other elements are zero.

The state of mmWave bandwidth allocation for all the mobile users in 5G cellular networks is composed of the following two components:

- The primary state component $\mathbb{B}$ describes the allocated bandwidth to all the users $\mathcal{U}$ in the whole area $\mathcal{S}$;
- The random state component $\mathbb{W}$ describes the movement of a particular user among different regions.

Therefore, the state space $\mathcal{D}$ composed of all possible combinations of the primary state component and random state component can be given by

$$\mathcal{D} = \{i = (\mathbb{B}, \mathbb{W}) \mid \mathbb{B} \in \mathcal{B}, \mathbb{W} \in \mathcal{W}\} \tag{7}$$

where $\mathcal{B}$ is the set of all bandwidth allocation solutions based on the available rates $\mathbb{R}_{\boldsymbol{s}}$ in each region, and $\mathcal{W}$ is the set of all events consisting of a single user moving from one region to another.

Remark: When a user U_n moves from region $\boldsymbol{s}$ to $\boldsymbol{s}'$, described by matrix $\mathbb{W}$, there would be new bandwidth allocated to U_n in region $\boldsymbol{s}'$. Thus, the system state transition occurs when a single user moving from one region to another.

The time duration for the user U_n staying in region $\boldsymbol{s}$ until it moves to region $\boldsymbol{s}'$ is independent of the previous visit regions and the previous length of connection, and is exponentially distributed with rate $\xi_{n\boldsymbol{s}\boldsymbol{s}'}$. The probability that a mobile user U_n currently in region $\boldsymbol{s}$ moves to region $\boldsymbol{s}'$ is independent of the regions U_n has already visited and is given to be $\boldsymbol{q}_{n\boldsymbol{s}\boldsymbol{s}'}$ with $\sum_{\boldsymbol{s}'} \boldsymbol{q}_{n\boldsymbol{s}\boldsymbol{s}'} = 1$. Thus, the arrival of the random event that a user changes its region is a Poisson process with rate of $\boldsymbol{q}_{n\boldsymbol{s}\boldsymbol{s}'}\xi_{n\boldsymbol{s}\boldsymbol{s}'}$. The process of all the users moving in the whole area is the combination of the independent Poisson processes. Based on these assumptions, the next state $j = (\mathbb{B}, \mathbb{W})$ only depends on the current state i and the allocated bandwidth for the user moving into the new region, i.e., Markov property.

This paper considers the general cases that the knowledge of where a particular user U_n is heading or the history of U_n's locations are unavailable. However, our methodology extends to cases where such information is available. The statistical parameters regarding these information, such as $\boldsymbol{q}_{n\boldsymbol{s}\boldsymbol{s}'}$ and $\xi_{n\boldsymbol{s}\boldsymbol{s}'}$, can be obtained either through measurements or other means. Since we consider the bandwidth allocation problem for existing mobile users in 5G cellular networks, the admission control for new arrivals and user departures of the system are beyond the scope of this paper.

B. The Control Space

For each state $i = (\mathbb{B}, \mathbb{W}) \in \mathcal{D}$, the control set $A(i)$ is the available rate set in the region $\boldsymbol{s}'$ for new user U_n moving into region $\boldsymbol{s}'$. Specifically, $A(i) = \mathbb{R}_{\boldsymbol{s}'} = \left\{\frac{1}{\mathcal{K}}R_{\boldsymbol{s}'}, \frac{2}{\mathcal{K}}R_{\boldsymbol{s}'}, \ldots, R_{\boldsymbol{s}'}\right\}$ if $w_{n,\boldsymbol{s}'} = 1$ with $w_{n,\boldsymbol{s}'} \in \mathbb{W} \in i$. Therefore, the control space is

$$\mathcal{A} = \bigcup_{i\in\mathcal{D}} A(i) = \bigcup_{\boldsymbol{s}'\in\mathcal{S}} \mathbb{R}_{\boldsymbol{s}'} \tag{8}$$

Given the state i with the random component $\mathbb{W}$ describing user's movement from region $\boldsymbol{s}$ to region $\boldsymbol{s}'$, the control of state

i determines a selected rate from the set of available rates $\mathbb{R}_{s'}$ in region s'. The selected rate is the newly allocated bandwidth to the user U_n moving into region s'.

The selected rate for each user passing different regions has significant impact on the playout quality of multimedia applications. Specifically, if the packet arrival rate into the buffer (which can be translated from the selected rate) is less than the packet departure rate, the playout buffer would be discharged and it is possible that the video is frozen when the buffer is empty. The larger allocated bandwidth can smooth the playout quality and charge the buffer, while it would result in less bandwidth allocated to other users in the same region, which causes frozenness for other users. Therefore, how to select the bandwidth from available rate set for the users going through different regions to optimize the playout quality of all the users is a challenging and important issue. Note that all the possible controls would be zero if mmWave signal is unavailable in region s'.

C. The State Transition Probabilities

For any bandwidth allocation configuration $\mathbb{B}$, the time duration until the next random event $\mathbb{W}$ occurs depends on the movements of all the users in the network. For each user, the arrival of random event is a Poisson process with rate of $\boldsymbol{q}_{nss'}\xi_{nss'}$. The overall rate $\Lambda_{\mathbb{B}}$ at which random events occur starting from a bandwidth allocation configuration $\mathbb{B}$ is the sum of the rates of all possible events and is given by

$$\Lambda_{\mathbb{B}} = \sum_{n=1}^{\mathcal{N}} \sum_{s\in\mathcal{S}} \sum_{s'\in\mathcal{S}} \mathrm{I}_{n,s}\boldsymbol{q}_{nss'}\xi_{nss'} \tag{9}$$

where $\mathrm{I}_{n,s}$ indicates if user U_n is in the sth region and defined as

$$\mathrm{I}_{n,s} = \begin{cases} 1, & (U_n \text{ in } \boldsymbol{s}) \\ 0, & (\text{otherwise}) \end{cases} \tag{10}$$

Assuming the control takes effect immediately, the total state transition rate from state i under control $a \in A(i)$ to next state is then $\Lambda_{\mathbb{B}}$. We denote the expected time duration of the transition from state i under control a to the next state as $\overline{\tau}_i(a)$

$$\overline{\tau}_i(a) = \frac{1}{\Lambda_{\mathbb{B}}} \tag{11}$$

For state i, given the random state component $\mathbb{W}^{(i)}$ with $w^{(i)}_{n,s} = -1$ and $w^{(i)}_{n,s'} = 1$, the primary state component $\mathbb{B}^{(i)}$, and the control $a \in A(i) = \mathbb{R}_{s'} = \left\{\frac{1}{\mathcal{K}}R_{s'}, \frac{2}{\mathcal{K}}R_{s'}, \ldots, R_{s'}\right\}$, the next primary state component $\mathbb{B}^{(j)} = \|B_{\widehat{n},\widehat{s}}\|_{\mathcal{N}\times S}$ can be given as

$$B^{(j)}_{\widehat{n},\widehat{s}} = \begin{cases} a * w^{(i)}_{n,s'}, & (\widehat{n} = n, \widehat{s} = s') \\ B^{(i)}_{n,s}\left(1 + w^{(i)}_{n,s}\right), & (\widehat{n} = n, \widehat{s} = s) \\ B^{(i)}_{\widehat{n},\widehat{s}}, & (\text{otherwise}). \end{cases} \tag{12}$$

The probability distribution of the next random event $\mathbb{W}^{(j)}$ depends on the bandwidth allocation configuration resulting from the current state i and control $a \in A(i)$. Given $\mathbb{B}^{(j)}$ by (12), the state transition probability from state $i = (\mathbb{B}^{(i)}, \mathbb{W}^{(i)}) \in \mathcal{D}$ to state $j = (\mathbb{B}^{(j)}, \mathbb{W}^{(j)}) \in \mathcal{D}$ is the rate at which the event occurs divided by the total transition rate:

$$p(j \mid i, a) = p_{i,j}(a) = \frac{1}{\Psi} \frac{\mathrm{I}_{n,s}\boldsymbol{q}_{nss'}\xi_{nss'}}{\sum_{n=1}^{\mathcal{N}} \sum_{s\in\mathcal{S}} \sum_{s'\in\mathcal{S}} \mathrm{I}_{n,s}\boldsymbol{q}_{nss'}\xi_{nss'}} \tag{13}$$

where $1/\Psi$ is the probability of selecting one rate from Ψ available rates in region s' if region s' is double-coverage area with $R_{s'} > 0$. Ψ is maximum integer within the range of $0 \le \Psi \le \mathcal{K}$ satisfying the capacity constraint of mmWave base station. Specifically, assuming the moving-in region s' is within the coverage of mmWave base station B_m, Ψ is the maximum k satisfying the constraint of

$$\left(\sum_{s\in B_m} \sum_{n=1}^{\mathcal{N}} B_{n,s}\right) - B_{n,s} + \frac{k}{\mathcal{K}}R_{s'} \le C_m \tag{14}$$

if the moving-out region s and the moving-in region s' are within the same mmWave base station B_m. Otherwise, if only the moving-in region s' is within the coverage of mmWave base station B_m, the constraint should be

$$\left(\sum_{s\in B_m} \sum_{n=1}^{\mathcal{N}} B_{n,s}\right) + \frac{k}{\mathcal{K}}R_{s'} \le C_m. \tag{15}$$

For the scenario that the moving-in region s' is single-coverage area, the only control we can select is $a = 0$. Thus, the state transition probability is

$$p(j \mid i, a) = p_{i,j}(a) = \frac{\mathrm{I}_{n,s}\boldsymbol{q}_{nss'}\xi_{nss'}}{\sum_{n=1}^{\mathcal{N}} \sum_{s\in\mathcal{S}} \sum_{s'\in\mathcal{S}} \mathrm{I}_{n,s}\boldsymbol{q}_{nss'}\xi_{nss'}} \tag{16}$$

with $R_{s'} = 0$.

Remark: As shown in (13) and (16), the state transition probability is a function of the probability $\boldsymbol{q}_{nss'}$. The state transition probability for a user moving to non-neighboring regions would be zero if we assume a user can only move to its neighboring regions, i.e., $\boldsymbol{q}_{nss'} = 0$ if s' is not a neighboring region of s.

D. The Cost Function

The objective is to properly select controls at each state to maximize the playout quality, which is the smooth playout duration over the whole transmission period for all the users in the network under the capacity constraint of each mmWave base station B_m. To evaluate the smoothness of multimedia applications at the user, we define ***quality consistency*** as the percentage of time when there is no frozenness or/and no packet dropping at the user out of the total operation period of video traffic.

With the proposed buffer system, there are $\mathcal{N}$ queues in the system with each queue corresponding to one user. Fig. 3 shows the timing structure of the system and recursive queuing model for the user U_n with packet arrivals, departures, and queue state. The timing of the whole system is divided into stages. Each stage is characterized by a specific state. The system is in

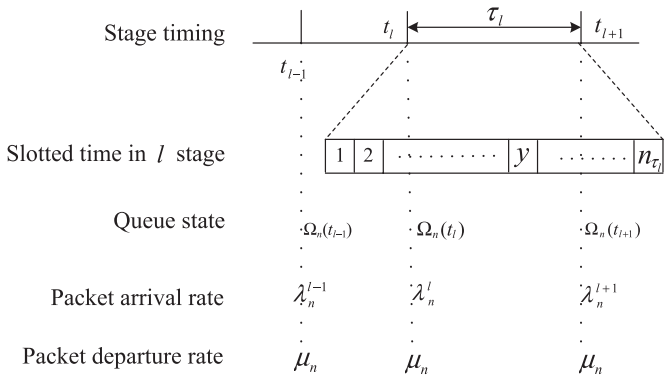

Fig. 3. The recursive queue model for user n.

the same stage until state transition occurs. A new stage starts (previous stage ends at the same time) when the system enters a new state with any user moving into a new region. We need to allocate a new bandwidth for the user moving from previous region to new region. In other words, in each stage, all the users utilize the same bandwidths as those in previous stage except for the user triggering the new stage. Let t_l denote the starting time of the lth stage of the MDP, thus $\tau_l = (t_{l+1} - t_l)$ is the duration for the lth stage. Time set $\mathcal{T} = \{t_1, t_2, \ldots, t_l, \ldots, t_L\}$ indicates the starting time for each stage where L is the total number of stages. For the lth stage corresponding to the state with user U_n moving from region $\boldsymbol{s}$ to region $\boldsymbol{s}'$, the stage duration can be given as

$$\tau_l = \frac{1}{\xi_{n\boldsymbol{s}\boldsymbol{s}'}} \tag{17}$$

The queue state at the beginning of each stage is used in the cost function as shown in the following of the paper. Therefore, we recursively derive the queue state based on the slotted time structure resulting from TDMA-based MAC in mmWave networks. As shown in Fig. 3, there are n_{τ_l} time slots during the lth stage and each time slot has a fixed duration T with $\tau_l = Tn_{\tau_l}$. It is assumed that the packets move out of the queue at the beginning of each time slot and the arriving packets enter the queue throughout the time slot. For user U_n in the yth time slot of the lth stage, let $\Upsilon_n^{(l)}(y)$ denote the number of packets left in the queue after $V_n^{(l)}(y)$ packets move out of the queue, then we have

$$\Upsilon_n^{(l)}(y) = \max\left\{0, \Omega_n^{(l)}(y-1) - V_n^{(l)}(y)\right\} \tag{18}$$

where $\Omega_n^{(l)}(y-1)$ is the queue length for user U_n at the end of the $(y-1)$th time slot. The number of free slots in the queue at the beginning of yth slot is thus:

$$\begin{aligned} F_n^{(l)}(y) &= G - \Upsilon_n^{(l)}(y) \\ &= G - \max\left\{0, \Omega_n^{(l)}(y-1) - V_n^{(l)}(y)\right\}. \end{aligned} \tag{19}$$

where G is the buffer size. If the number of arriving packets in the yth slot $A_n^{(l)}(y)$ is larger than $F_n^{(l)}(y)$, only $F_n^{(l)}(y)$ packets enter the queue and the other $[A_n^{(l)}(y) - F_n^{(l)}(y)]$ packets are dropped. Therefore, the recursion of the queue state can be given as follows,

$$\Omega_n^{(l)}(y) = \min\left\{G, \max\left\{0, \Omega_n^{(l)}(y-1) - V_n^{(l)}(y)\right\} + A_n^{(l)}(y)\right\}. \tag{20}$$

Based on the recursion (20), we can obtain the queue state $\Omega_n(t)$ for the user U_n at anytime t corresponding to the yth time slot in lth stage, which can be defined as

$$\Omega_n(t) \triangleq \Omega_n^{(l)}(y), \text{ with } t \geq 0. \tag{21}$$

$\Omega_n(t)$ can be affected by the initial queue state and the packet arrival/departure rates. It is known that the packet delay mainly results from the randomness of packet arrival and departure [28]. Since the emerging high-rate video applications have stringent requirements on delay and data rate, massive packets come intensively to the buffer with much lower randomness. Taking into account the fact that the scale of stage duration is much larger than the scale of packet randomness, the randomness of packet arrival and departure is not considered in the cost of each stage, in order to make the analysis tractable. Let $\mathbb{X}(t)$ represent the state for the system at time t with $\mathbb{X}(t) = (\mathbb{B}^{(t)}, \mathbb{W}^{(t)}) \in \mathcal{D}$, and $a(t)$ represents the control at time t for state $\mathbb{X}(t)$ with $a(t) \in \mathcal{A}$. The allocated bandwidth for user U_n in the lth stage can be obtained from $\mathbb{X}(t)$ and $a(t)$. Specifically, $\mathbb{B}^{(t)}$ describes the allocated bandwidth for each user in different regions; $\mathbb{W}^{(t)}$ determines the user to re-select the allocated bandwidth; and the control $a(t)$ determines the new allocated bandwidth to the moving user selected by $\mathbb{W}^{(t)}$. Let $\lambda_n^{(l)}$ denote the packet arrival rate of user U_n in the lth stage. $\lambda_n^{(l)}$ can be determined by the bandwidth allocation as follows:

$$\lambda_n^{(l)} = \begin{cases} a(t_l)/Z, & \left(\text{if } w_{n,\boldsymbol{s}}^{(t_l)} = 1 \text{ and } w_{n,\boldsymbol{s}'}^{(t_l)} = -1\right), \\ \sum\limits_{s \in \mathcal{S}} B_{n,s}^{(t_l)}/Z, & (\text{otherwise}). \end{cases} \tag{22}$$

where Z is the packet size.

The video application on each mobile user U_n has a specific data rate requirement r_n with $n \in \{1, 2, \ldots \mathcal{N}\}$. The packet departure rate for the nth queue does not depend on the stage and can be given as $\mu_n = r_n/Z$. With packet arrival rate $\lambda_n^{(l)}$, packet departure rate μ_n, and initial queue state $\Omega_n(t_l)$, the lth stage cost of user U_n (denoted by G_n^l) comes from the following two aspects:

- Quality loss duration is the total time duration when video quality loss results from the arrival packet dropping if the buffer is full;
- Frozenness duration is the total time duration when the video suffers from frozenness if there is no packets in the buffer for playout.

If $\lambda_n^{(l)} \geq \mu_n$, there is no frozenness duration for U_n in the lth stage and the stage cost is the quality loss duration. The time to fully charge the buffer in the lth stage (denoted by $t_c^{(l)}$) with initial buffer state $\Omega_n(t_l)$ is given as

$$t_c^{(l)} = \frac{G - \Omega_n(t_l)}{\lambda_n^{(l)} - \mu_n} \tag{23}$$

If the stage duration $\tau_l \leq \frac{G-\Omega_n(t_l)}{\lambda_n^{(l)}-\mu_n}$, there is no packet dropping and the stage cost $G_n^l = 0$. Otherwise, with the stage duration $\tau_l > \frac{G-\Omega_n(t_l)}{\lambda_n^{(l)}-\mu_n}$, the total number of dropping packets is $(\lambda_n^{(l)} - \mu_n)\left[\tau_l - \frac{G-\Omega_n(t_l)}{\lambda_n^{(l)}-\mu_n}\right]$. Thus, the stage cost in terms of quality loss duration is given as

$$G_n^l = \frac{\left(\lambda_n^{(l)} - \mu_n\right)\left[\tau_l - \frac{G-\Omega_n(t_l)}{\lambda_n^{(l)}-\mu_n}\right]}{\mu_n}. \tag{24}$$

If $\lambda_n^{(l)} < \mu_n$, there is no quality loss duration for U_n in the lth stage and the stage cost is the frozenness duration. The time to fully discharge the buffer in the lth stage (denoted by $t_d^{(l)}$) with initial buffer state $\Omega_n(t_l)$ is given as

$$t_d^{(l)} = \frac{\Omega_n(t_l)}{\mu_n - \lambda_n^{(l)}} \tag{25}$$

If the stage duration $\tau_l \leq \frac{\Omega_n(t_l)}{\mu_n-\lambda_n^{(l)}}$, there are always packets in the buffer to transmit and there is no frozenness duration in the lth stage with $G_n^l = 0$. Otherwise, with the stage duration $\tau_l > \frac{\Omega_n(t_l)}{\mu_n-\lambda_n^{(l)}}$, the total number of extra packets to be provided for smooth quality at user is $(\mu_n - \lambda_n^{(l)})\left[\tau_l - \frac{\Omega_n(t_l)}{\mu_n-\lambda_n^{(l)}}\right]$. Thus, the stage cost in terms of frozenness duration is given as

$$G_n^l = \frac{\left(\mu_n - \lambda_n^{(l)}\right)\left[\tau_l - \frac{\Omega_n(t_l)}{\mu_n-\lambda_n^{(l)}}\right]}{\mu_n}. \tag{26}$$

Therefore, the stage cost of user U_n in the lth stage can be summarized as

$$G_n^l = \begin{cases} \frac{\left(\lambda_n^{(l)}-\mu_n\right)\left[\tau_l-\frac{G-\Omega_n(t_l)}{\lambda_n^{(l)}-\mu_n}\right]}{\mu_n}, & \left(\lambda_n^{(l)} \geq \mu_n,\ \tau_l > \frac{G-\Omega_n(t_l)}{\lambda_n^{(l)}-\mu_n}\right), \\ 0, & \left(\lambda_n^{(l)} \geq \mu_n,\ 0 < \tau_l \leq \frac{G-\Omega_n(t_l)}{\lambda_n^{(l)}-\mu_n}\right), \\ 0, & \left(\lambda_n^{(l)} < \mu_n,\ 0 < \tau_l \leq \frac{\Omega_n(t_l)}{\mu_n-\lambda_n^{(l)}}\right), \\ \frac{\left(\mu_n-\lambda_n^{(l)}\right)\left[\tau_l-\frac{\Omega_n(t_l)}{\mu_n-\lambda_n^{(l)}}\right]}{\mu_n}, & \left(\lambda_n^{(l)} < \mu_n,\ \tau_l > \frac{\Omega_n(t_l)}{\mu_n-\lambda_n^{(l)}}\right). \end{cases} \tag{27}$$

Our goal is to select a proper control at each possible state that minimizes the expected average cost per unit time. Given the set of initial queue state for all the users $\{\Omega_1(0), \Omega_2(0), \ldots, \Omega_{\mathcal{N}}(0)\}$ and the set of required data rates $\{r_1, r_2, r_3, \ldots, r_{\mathcal{N}}\}$, we can obtain the stage costs for all the users in the whole process including L stages. Therefore, the objective cost function can be the sum of the stage costs of all the users over the total time as follows (P1):

$$\lim_{L\to\infty} \frac{1}{E(t_L)} \sum_{l=1}^{L} \sum_{n=1}^{\mathcal{N}} G_n^l. \tag{28}$$

Note that the objective function describes the average cost per unit time, resulting from the packet dropping and frozenness. The quality consistency can be obtained by $(1 - \text{P1})$. A policy ψ determines the controls for all the stages of P1. By minimizing P1, we can maximize the playout quality of all the users.

For mmWave 5G cellular networks with dense population, the bandwidth resources are not sufficient for all the users to achieve smooth playout quality. Thus, the dominant cost in each stage is the frozenness duration. It is obvious that the optimal policy ψ^* for P1 will cause a biased solution, i.e., the bandwidth allocation would incline towards those users with lower required data rates while some unlucky users will suffer from lots of frozenness periods. To ensure long-term fairness among the competing users, a parameter ρ based on the weighted fair queuing [28] is adopted. The objective cost function can be given as (P2):

$$\lim_{L\to\infty} \frac{1}{E(t_L)} \sum_{l=1}^{L} \sum_{n=1}^{\mathcal{N}} \rho_n^{(l-1)} G_n^l. \tag{29}$$

where $\rho_n^{(l-1)}$ is the coefficient for G_n^l, obtained according to the bandwidth allocation records of previous $(l-1)$ stages for user U_n. Specifically, we have

$$\rho_n^{(l-1)} = \frac{\beta_n}{\left[\left(1 - g_n^{(l-1)}\right) + \epsilon\right]^{\alpha}} \tag{30}$$

where ϵ is a small positive scalar to prevent zero denominator, β_n is a weight for user U_n to provide differentiated services, and α is a parameter to make a tradeoff between fairness and total cost. $g_n^{(l-1)}$ is the average cost per unit time during the previous $(l-1)$ stages and is given as

$$g_n^{(l-1)} = \frac{\Sigma_{h=1}^{l-1} G_n^h}{\Sigma_{h=1}^{l-1} \tau_h} \tag{31}$$

With a large value of α, users with less accumulated smooth duration (calculated by $1 - g_n^{(l-1)}$) in the previous stages have larger values of ρ, so that they have less chance to obtain cost in the following stages. Thus, better fairness can be achieved. When $\alpha = 0$, the bandwidth resources are allocated to users without taking into account the history of the obtained cost.

V. Solving the MDP Model

In Section IV, we formulated the dynamic bandwidth allocation problem as an average cost Markov decision process, including the state space $\mathcal{D}$, the set of available controls $\mathcal{A}(i)$ for each state $i \in \mathcal{D}$, the state transition probabilities $p_{i,j}(a)$, and the cost function. In this section, we discuss how to solve the Markov decision progress with dynamic programming method.

A. Bellman's Equation

Bellman's Equation is an effective dynamic programming method to solve the MDP problem achieving optimality [31]. Given any stationary policy ψ, $\psi(i) \in A(i)$ is the control of state i. The average cost obtained by minimizing (28) or (29) under policy ψ is denoted by v^{ψ} while v^* is the average cost

under an optimal policy ψ^*. The average cost v^{ψ} is independent of the initial state for a stationary system. Consequently, we use "differential cost" to compare different states. The differential cost starting in state i under a policy ψ is denoted by $h^{\psi}(i)$ while the differential cost under an optimal policy ψ^* is $h^*(i)$. The optimal differential cost set $\vec{h}^* = \{h^*(i)|i \in \mathcal{D}\}$ and scalar v^* satisfy the Bellman's equation. Specifically, we have for all $i \in \mathcal{D}$

$$h^*(i) = \min_{a \in A(i)} \left\{ G(i,a) - v^* \overline{\tau}_i(a) + \sum_{j \in \mathcal{D}} p_{i,j}(a) h^*(j) \right\}, \quad (32)$$

where $G(i,a)$ is the stage cost corresponding to state i and is given as

$$G(i,a) = \sum_{n=1}^{\mathcal{N}} G_n^{(i)}. \quad (33)$$

Given the optimal average cost v^* and the optimal differential cost set $\vec{h}^* = \{h^*(i)|i \in \mathcal{D}\}$, the optimal control $\psi(i)$ can be obtained by minimizing the current stage cost minus the expected average cost of the stage plus the remaining expected differential cost based on the possible resulting states, i.e., for all $i \in \mathcal{D}$

$$\psi^*(i) = \arg \min_{a \in A(i)} \left\{ G(i,a) - v^* \overline{\tau}_i(a) + \sum_{j \in \mathcal{D}} p_{i,j}(a) h^*(j) \right\}. \quad (34)$$

Specifically, if the instantaneous rate in the destination region $\boldsymbol{s}'$ is $R_{\boldsymbol{s}'} \neq 0$, we have for all $i \in \mathcal{D}$

$$\psi^*(i) = \arg \min_{a \in \mathbb{R}_{\boldsymbol{s}'}} \left\{ G(i,a) - v^* \overline{\tau}_i(a) + \sum_{j \in \mathcal{D}} p_{i,j}(a) h^*(j) \right\}; \quad (35)$$

Otherwise, the destination region is single-coverage area with $R_{\boldsymbol{s}'} = 0$ and there is no control to exercise, i.e.,

$$\psi^*(i) = 0. \quad (36)$$

Several methods can be used to obtain the optimal average cost v^* and the optimal differential cost set $\vec{h}^* = \{h^*(i)|i \in \mathcal{D}\}$ [31]. In this paper, we adopt the iteration method to achieve optimal v^* and $\vec{h}^*$. Initially, we set $v_0^* = 0$ and $\vec{h}_0^* = \mathbf{0}$. For the βth iteration step, each $h_\beta^*(i)$ for all $i \in \mathcal{D}$ and v_β^* are calculated according to (32) based on the newly obtained values by traversing all the possible controls of state i. If the obtained control set in the βth iteration step is the same as that of the $(\beta-1)$th iteration step, the iteration is considered to be converged and the achieved v_β^* and $\vec{h}_\beta^*$ are the optimal values.

The computational complexity of the iteration algorithm is $O(\|A\|\|\mathcal{D}\|^2)$ [32], where $\|.\|$ is the cardinality of a set. The number of controls for each state i is the number of available rates in the moving-in region $\boldsymbol{s}'$. Thus the total number of controls in the control space $\mathcal{A}$ is $\|\mathcal{A}\| \approx \mathcal{K}S$. Each state $i \in \mathcal{D}$ is determined by both $\mathbb{B}^{(i)}$ and $\mathbb{W}^{(i)}$. $\mathbb{B}^{(i)}$ describes the location of $\mathcal{N}$ users among S regions and the allocated bandwidth for each user with $\|\mathbb{B}^{(i)}\| \approx S^{\mathcal{N}}\mathcal{K}^{\mathcal{N}}$. $\mathbb{W}^{(i)}$ determines the moving user from $\mathcal{N}$ users and the moving-in/moving-out regions with $\|\mathbb{W}^{(i)}\| \approx \mathcal{N}S(S-1)$. The cardinality of $\mathcal{D}$ is $\|\mathcal{D}\| \approx S^{\mathcal{N}}\mathcal{K}^{\mathcal{N}}\mathcal{N}S(S-1) = S^{\mathcal{N}+1}\mathcal{K}^{\mathcal{N}}\mathcal{N}(S-1)$. Therefore, the computational complexity of the iteration algorithm to obtain the optimal v^* and $\vec{h}^*$ is

$$\begin{aligned} O\left(\|A\|\|\mathcal{D}\|^2\right) &\approx O\left(\mathcal{K}S\left\{S^{\mathcal{N}+1}\mathcal{K}^{\mathcal{N}}\mathcal{N}(S-1)\right\}^2\right) \\ &\approx O(\mathcal{K}^{2\mathcal{N}+1}S^{2\mathcal{N}+5}\mathcal{N}^2) \end{aligned} \quad (37)$$

From (37), it is shown that the iteration algorithm to obtain optimal v^* and $\vec{h}^*$ introduces extremely high computational complexity. The computation can be done off-line with high-speed computer systems (which are separate and independent of the real system), before the real system starts to operate. Once the iterations are completed, the optimal decision at each stage can be determined quickly according to Bellman's equation. However, even off-line computation, the iteration complexity required to determine the optimal average cost v^* and the optimal differential cost set $\vec{h}^*$ is overwhelming due to the exponential complexity as shown in (37). As a result, lower-complexity method is necessary. In Section V-B, approximation method is used to significantly reduce the complexity by reducing the number of states taking into account the unique characteristics of mmWave network.

B. An Approximate Solution

Equation (37) shows that the iteration complexity greatly depends on the number of mobile users $\mathcal{N}$ in the system, the number of available rates $\mathcal{K}$ in each region, and the number of regions S of the whole area. In this section, we give an approximate solution for the MDP problem by reducing the number of regions S and the number of available rates $\mathcal{K}$ in each region, given the number of mobile users $\mathcal{N}$.

In 5G cellular networks, mmWave base stations are likely to be densely deployed in small cell to provide high capacity to satisfy the demand of ultra-high traffic volume density. In addition, mmWave communication range is confined due to the severe propagation loss in mmWave frequency band. Therefore, the transmission range of mmWave communication in 5G cellular networks is relatively shorter than the range of previous generations of cellular networks. According to (1), the shorter transmission distance results in less differences on the path loss over distance and so does the transmission data rate. Thus, the whole double-coverage region is considered to have uniform instantaneous data rate of mmWave transmission denoted by $R_{\boldsymbol{d}}$, where the subscript $\boldsymbol{d}$ indicates the double-coverage region. Therefore, the whole single-coverage area (or the whole double-coverage area) is considered to be a single region since each region has the same instantaneous transmission rate. In the whole 5G coverage area, there are only two regions, namely, single-coverage region and double-coverage region. With the simplifications on instantaneous transmission rate, the total number of regions is reduced from S to 2 by considering mmWave propagation characteristics. With above approximations, the set of regions in the whole area is $\mathcal{S} = \{\boldsymbol{s}, \boldsymbol{d}\}$

and the available rate set in double-coverage area is $\mathbb{R}_{\boldsymbol{d}}$. For each state $i = (\mathbb{B}, \mathbb{W}) \in \mathcal{D}$, $\mathbb{B}$ is simplified as

$$\mathbb{B} = \begin{Vmatrix} B_{1,\boldsymbol{s}} & B_{1,\boldsymbol{d}} \\ B_{2,\boldsymbol{s}} & B_{2,\boldsymbol{d}} \\ \vdots & \vdots \\ B_{\mathcal{N},\boldsymbol{s}} & B_{\mathcal{N},\boldsymbol{d}} \end{Vmatrix} = \begin{Vmatrix} 0 & B_{1,\boldsymbol{d}} \\ 0 & B_{2,\boldsymbol{d}} \\ \vdots & \vdots \\ 0 & B_{\mathcal{N},\boldsymbol{d}} \end{Vmatrix} \tag{38}$$

where $B_{n,\boldsymbol{d}} \in \mathbb{R}_{\boldsymbol{d}}$ if user U_n is in double-coverage region while $B_{n,\boldsymbol{d}} = 0$ if user U_n is in single-coverage region; $\mathbb{W}$ can be simplified as

$$\mathbb{W} = \begin{Vmatrix} w_{1,\boldsymbol{s}} & w_{1,\boldsymbol{d}} \\ \vdots & \vdots \\ w_{n,\boldsymbol{s}} & w_{n,\boldsymbol{d}} \\ \vdots & \vdots \\ w_{\mathcal{N},\boldsymbol{s}} & w_{\mathcal{N},\boldsymbol{d}} \end{Vmatrix} = \begin{Vmatrix} 0 & 0 \\ \vdots & \vdots \\ w_{n,\boldsymbol{s}} & w_{n,\boldsymbol{d}} \\ \vdots & \vdots \\ 0 & 0 \end{Vmatrix} \tag{39}$$

where $w_{n,\boldsymbol{s}} = 1$ and $w_{n,\boldsymbol{d}} = -1$ if user U_n moves from double-coverage region to single-coverage region while $w_{n,\boldsymbol{s}} = -1$ and $w_{n,\boldsymbol{d}} = 1$ if user U_n moves from single-coverage region to double-coverage region.

The iteration complexity shown in (37) can be further reduced if we choose the control for each state from less number of available rates in the double-coverage region. The number of available rates in the double-coverage region determines the fineness of bandwidth allocation. In the MDP model in Section IV, the available rates depend on the number of time slots in each superframe, i.e., the available rate set in double-coverage area is $\left\{\frac{1}{\mathcal{K}}R_{\boldsymbol{d}}, \frac{2}{\mathcal{K}}R_{\boldsymbol{d}}, \ldots, R_{\boldsymbol{d}}\right\}$. In the approximate solution, we adopt larger fineness of rate selection, i.e., the available rate set is $\mathbb{R}_{\boldsymbol{d}} = \left\{\frac{\eta}{\mathcal{K}}R_{\boldsymbol{d}}, \frac{2\eta}{\mathcal{K}}R_{\boldsymbol{d}}, \ldots, \frac{Q\eta}{\mathcal{K}}R_{\boldsymbol{d}}\right\}$ with $Q = \left\lfloor \frac{\mathcal{K}}{\eta} \right\rfloor$ where $\eta \gg 1$. Thus the number of available rates in the double-coverage region can be reduced from $\mathcal{K}$ to Q. The simplified control space is $\mathcal{A} = A(s) \cup A(d) = \left\{0, \frac{\eta}{\mathcal{K}}R_{\boldsymbol{d}}, \frac{2\eta}{\mathcal{K}}R_{\boldsymbol{d}}, \ldots, \frac{Q\eta}{\mathcal{K}}R_{\boldsymbol{d}}\right\}$.

For the case that 20 users move in the area with 100 regions, the iteration complexity after simplification is $1/(2^{86}5^{136})$ of the original iteration complexity if 10 rates are available for the users to select in double-coverage region. In the approximation solution, we consider the case that all the users are uniformly distributed in the whole area, thus the capacity constraint is for all the users in the whole coverage area. The optimal policy can be obtained by Bellman's equation based on the MDP model described in Section IV-C and D with the simplified states.

C. Implementation Considerations

To implement the proposed method on video quality provisioning, there is a controller connected with all the mmWave base stations in the coverage area. In each mmWave base station, there is an index table saving the information of each state and the corresponding control obtained by off-line calculation with Bellman's equation. When a user U_n enters the new region, the associated mmWave base station determines the new state based on previous state and the moving-in region of the user U_n. Then, the associated mmWave base station allocates the bandwidth to the user U_n immediately according to the index table. The movement of the user U_n is reported to the controller by the associated mmWave base station. The controller broadcasts the new state to all the mmWave base stations and the whole system waits for another user entering the new region to trigger the incoming new state. Note that there is only one user with mmWave bandwidth re-allocation when system enters a new state and other users have the same bandwidth allocations as the previous state. The user entering a new region can obtain the newly allocated bandwidth immediately and does not need to wait for the updated information from the controller to start bandwidth allocation.

VI. Numerical Results

In this section, numerical results are provided to demonstrate the performance of the bandwidth allocation solution obtained from the MDP model with state aggregation, compared with another two solutions, namely random policy solution and normal transmission solution. Random policy solution is based on the proposed buffer system and randomly selects the allocated bandwidth of the user among available rates in each MDP stage. In normal transmission solution, the buffer system is not installed in the user to mitigate the effect of link outage and the allocated bandwidth for each user is based on the required data rate of video applications. The performance of the obtained optimal policy with state aggregation is mainly demonstrated by quality consistency. Additionally, we show the distribution of the frozenness duration, the impact of buffer size on quality consistency, and the number of supported traffic in mmWave network.

The numerical results are conducted in a square area with side length of 10 Km. Initially, a number of users are randomly located in the whole area with none packets in each buffer. mmWave base stations are distributed in the whole area in grid topology with the distance of 500 m. The instantaneous data rate in double-coverage region is estimated by

$$R \approx W \log_2 \left[1 + \frac{P_T G_R G_T \lambda^2}{16\pi^2 (N_0 + I) W d^n}\right] \tag{40}$$

where P_T is the transmitted power, G_T and G_R are respectively the antenna gains of the transmitter and receiver. λ is the wavelength, W is the system bandwidth, N_0 and I are the one-side power spectral densities of white Gaussian noise and broadband interference, respectively. d is the transmission distance and the maximum link operation range is adopted for link budget to determine the instantaneous rate in the double-coverage area. The propagation-related parameters are shown in Table II.

The time durations of each user staying in single-coverage region and double-coverage region are exponentially distributed with rate $\xi_{n\boldsymbol{sd}}$ and $\xi_{n\boldsymbol{ds}}$, respectively. Each $\xi_{n\boldsymbol{sd}}$ for user U_n is randomly selected within the range of $\left[\frac{1}{15}, \frac{1}{30}\right]$ while each $\xi_{n\boldsymbol{ds}}$ for user U_n is also randomly selected within the range of $\left[\frac{1}{80}, \frac{1}{120}\right]$. The required data rate of the multimedia application in each user is randomly selected from the range of [1.5 Gbps, 2 Gbps]. The system-related parameters are shown in Table III.

TABLE II
PROPAGATION RELATED PARAMETERS

Parameters	Value
Central frequency (f)	30 GHz
Spectrum bandwidth (W)	2 GHz
Transmission power (P_T)	0.5mW
Background noise (N_0)	-134dBm/MHz
Maximum distance (d)	250 m
Link outage threshold (PL_{thr})	-40 dBm
Transmitter antenna gain (G_T)	1
Receiver antenna gain (G_R)	1

TABLE III
SYSTEM RELATED PARAMETERS

Parameters	Value
Packet size (Z)	10^3 bits
Buffer size (G)	16×10^6 packets
Capacity of double-coverage region	200 Gbps
Number of available rates (Q)	10
Time slot duration	$18\mu s$

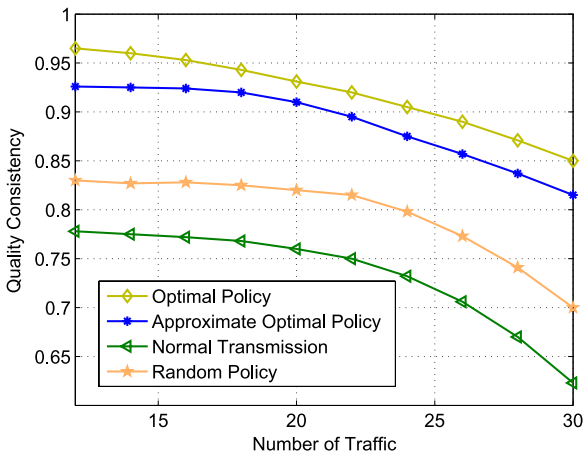

Fig. 4. Quality consistency via the number of traffics.

A. Quality Consistency

Fig. 4 shows the numerical results on quality consistency of the four solutions with various numbers of video traffic. The optimal policy and approximate solution achieve much better quality consistency than random policy and normal transmission. As more traffic is involved, the quality consistency goes down when the total allocated bandwidth reaching the system capacity. By allocating more bandwidth than the required bandwidth to the users in the double-coverage region, the stored data in the buffer can be used to maintain video playout quality in single-coverage region. The proposed buffer system can mitigate the impact of link outage on video playout quality at the cost of the storage space and extra bandwidth.

Fig. 5 shows the impact of buffer size on maintaining quality consistency for both approximate solution and random policy solution. It is shown that as buffer size increases, the quality consistency can be improved. Large buffer size has the robustness on allocated bandwidth of each user to improve quality

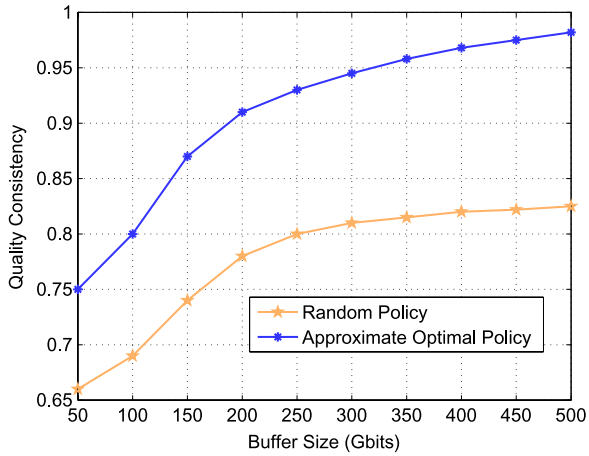

Fig. 5. Quality consistency of different buffer sizes.

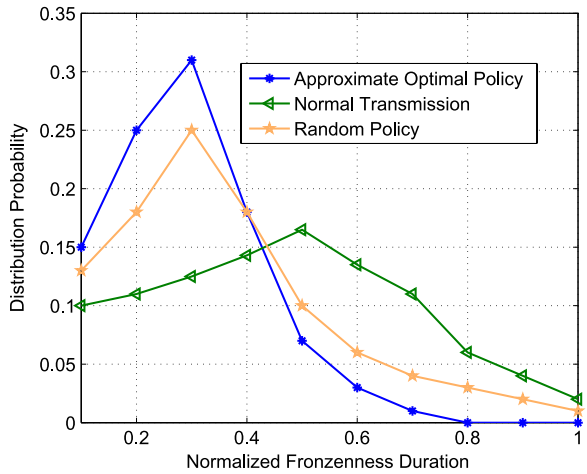

Fig. 6. Probability distribution of frozenness duration.

consistency. Specifically, on one hand, large buffer has lower probability to be overflowed, which results in lower packet dropping probability; On the other hand, large buffer can store more packets for users spending longer time in single-coverage area without suffering from frozenness. The extreme case is that we can achieve 100 percentages quality consistency for a stationary system if we use infinite buffer at the user and allocate very high bandwidth to each user.

B. Frozen Duration Distribution

Fig. 6 shows the probability distribution of the normalized frozenness period suffered by all the users in the network. The probability distribution of frozenness duration shows that the obtained approximate solution with buffer system can greatly reduce the frozenness duration compared with the other two solutions, since most of the frozenness durations in approximate solution are in the short duration range. The proposed method using dynamic bandwidth allocation to maintain video quality is very effective when mmWave links suffering from frequent link outage. The random policy solution can reduce the frozenness duration compared with normal transmission solution because of the buffer system.

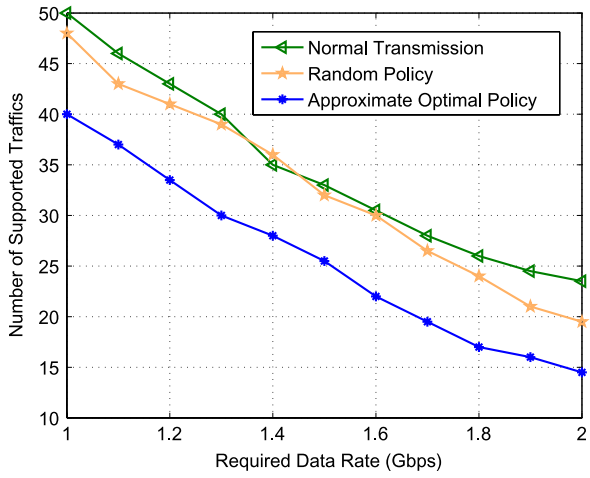

Fig. 7. Number of supported traffic.

C. Number of Supported Traffic

The number of traffic supported successfully in the network based on the required bandwidth is shown in Fig. 7. It can be seen that the network with approximate solution can support less number of traffic than that in normal transmission solution since larger bandwidth need to be allocated to users for video quality provisioning. Both the video frozenness duration and the probability of video frozenness can be significantly reduced at the cost of extra allocated bandwidth.

VII. Conclusion and Future Research

In this paper, we dealt with video quality provisioning problem for mobile users in mmWave 5G cellular networks by bandwidth allocation. The problem of dynamic bandwidth allocation in mmWave band for users alternatively entering single-coverage region and double-coverage region is formulated as an MDP model. By solving the MDP model, we can obtain the optimal policy indicating the allocated bandwidth to each user in different regions. The obtained optimal policy can dynamically charge or discharge the buffer to maintain the video playout quality at the user. The numerical results demonstrate that the proposed methodology on video playout quality provisioning can effectively mitigate the impact of frequent mmWave link outage and significantly improve the smoothness of video quality.

The proposed method on playout quality provisioning is effective for non-real time video applications of the users with high mobility. For low-mobility users, it is possible that the users stay in the areas with mmWave link outage for much longer time. In this case, multi-hop relaying [20], [30] is likely an effective method to maintain network connectivity by replacing the outage link with multiple available links. Longer setup time of multi-hop relaying has less impact on network performance since it does not require frequent path re-selections for low-mobility scenarios. Real-time multimedia applications of high-mobility users can be supported by switching the underlaying network from mmWave to 4G to overcome frequent mmWave link outage problem. However, in this case, the playout quality of multimedia applications would descend because of the lower transmission rate of 4G network.

References

[1] T. S. Rappaport *et al.*, "Millimeter wave mobile communications for 5G cellular: It will work!" *IEEE Access*, vol. 1, pp. 335–449, May 2013.
[2] Z. Pi and F. Khan, "An introduction to millimeter-wave mobile broadband systems," *IEEE Commun. Mag.*, vol. 49, no. 6, pp. 101–107, Jun. 2011.
[3] J. Qiao, X. Shen, J. W. Mark, Q. Shen, and L. Lei, "Enabling device-to-device communication in millimeter wave 5G cellular networks," *IEEE Commun. Mag.*, vol. 53, no. 1, pp. 209–215, Jan. 2015.
[4] J. G. Andrews *et al.*, "What will 5G be?" *IEEE J. Sel. Areas Commun.*, vol. 32, no. 6, pp. 1065–1082, Jun. 2014.
[5] M. R. Akdeniz *et al.* "Millimeter wave channel modeling and cellular capacity evaluation," *IEEE J. Sel. Areas Commun.*, vol. 32, no. 6, pp. 1164–1179, Jun. 2014.
[6] L. X. Cai, L. Cai, X. Shen, and J. W. Mark, "REX: A randomized exclusive region based scheduling scheme for mmWave WPANs with directional antenna," *IEEE Trans. Wireless Commun.*, vol. 9, no. 1, pp. 113–121, Jan. 2010.
[7] F. Gutierrez, S. Agarwal, K. Parrish, and T. S. Rappaport, "On-chip integrated antenna structures in CMOS for 60 GHz WPAN systems," *IEEE J. Sel. Areas Commun.*, vol. 27, no. 8, pp. 1367–1378, Oct. 2009.
[8] W. Roh *et al.*, "Millimeter-wave beamforming as an enabling technology for 5G cellular communications: Theoretical feasibility and prototype results," *IEEE Commun. Mag.*, vol. 52, no. 2, pp. 106–113, Feb. 2014.
[9] A. I. Sulyman *et al.*, "Radio propagation path loss models for 5G cellular networks in the 28 GHZ and 38 GHZ millimeter-wave bands," *IEEE Commun. Mag.*, vol. 52, no. 9, pp. 78–86, Sep. 2014.
[10] X. Pei, T. Jiang, D. Qu, G. Zhu, and J. Liu, "Radio resource management and access control mechanism based on a novel economic model in heterogeneous wireless networks," *IEEE Trans. Veh. Technol.*, vol. 59, no. 6, pp. 3047–3056, Jul. 2010.
[11] W. Song, H. Jiang, and W. Zhuang, "Performance analysis of the WLAN-first scheme in cellular/WLAN interworking," *IEEE Trans. Wireless Commun.*, vol. 6, no. 5, pp. 1932–1943, May 2007.
[12] W. Song, Y. Chen, and W. Zhuang, "Improving voice and data services in cellular/WLAN integrated network by admission control," *IEEE Trans. Wireless Commun.*, vol. 6, no. 11, pp. 4015–4037, Nov. 2007.
[13] D. Niyato and E. Hossain, "Bandwidth allocation in 4G heterogeneous wireless access networks: A noncooperative game theoretical approach," in *Proc. IEEE GLOBECOM*, Nov. 2006, pp. 1–5.
[14] M. Ismail and W. Zhuang, "A distributed multi-service resource allocation algorithm in heterogeneous wireless access medium," *IEEE J. Sel. Areas Commun.*, vol. 30, no. 2, pp. 425–432, Feb. 2012.
[15] D. Cavalcanti, D. Agrawal, C. Cordeiro, B. Xie, and A. Kumar, "Issues in integrating cellular networks, WLANs, and MANETs: A futuristic heterogeneous wireless network," *IEEE Wireless Commun.*, vol. 12, no. 3, pp. 30–41, Jun. 2005.
[16] A. Alshamrani, X. Shen, and L. Xie, "QoS provisioning for heterogeneous services in cooperative cognitive radio networks," *IEEE J. Sel. Areas Commun.*, vol. 29, no. 4, pp. 819–830, Apr. 2011.
[17] T. H. Luan, L. X. Cai, and X. Shen, "Impact of network dynamics on user's video quality: Analytical framework and QoS provision," *IEEE Trans. Multimedia*, vol. 12, no. 1, pp. 64–78, Jan. 2010.
[18] Y. Liu, L. Guo, F. Li, and S. Chen, "An empirical evaluation of battery power consumption for streaming data transmission to mobile devices," in *Proc. ACM Int. Conf. Multimedia*, Nov. 2011, pp. 473–482.
[19] J. He, Z. Xue, D. Wu, D. O. Wu, and Y. Wen, "CBM: Online strategies on cost-aware buffer management for mobile video streaming," *IEEE Trans. Multimedia*, vol. 16, no. 1, pp. 242–252, Jan. 2014.
[20] J. Qiao, L. X. Cai, X. Shen, and J. W. Mark, "Enabling multi-hop concurrent transmissions in 60 GHz wireless personal area networks," *IEEE Trans. Wireless Commun.*, vol. 10, no. 11, pp. 3824–3833, Nov. 2011.
[21] S. Singh, F. Ziliotto, U. Madhow, E. M. Belding, and M. J. W. Rodwell, "Millimeter wave WPAN: Cross-layer modeling and multihop architecture," in *Proc. IEEE INFOCOM*, May 2007, pp. 2336–2240.
[22] J. Qiao, X. Shen, J. W. Mark, and Y. He, "MAC-layer concurrent beamforming protocol for indoor millimeter wave networks," *IEEE Trans. Veh. Technol.*, vol. 64, no. 1, pp. 327–338, Jan. 2015.
[23] A. Maltsev, "Channel models for 60 GHz WLAN systems," IEEE 802.11-09/0334r8, May 2010.
[24] M. Jacob, C. Mbianke, and T. Kurner, IEEE doc. 802.11-09/1169r0. Human Body Blockage-Guidelines for TGad MAC development, Nov. 2009.

[25] S. Hur, T. Kim, J. V. Krogmeier, T. A. Thomas, and A. Ghosh, "Millimeter wave beamforming for wireless backhaul and access in small cell networks," *IEEE Trans. Commun.*, vol. 61, no. 10, pp. 4391–4403, Oct. 2013.
[26] C. Sum *et al.*, "Virtual time-slot allocation scheme for throughput enhancement in a millimeter-wave multi-Gbps WPAN system," *IEEE J. Sel. Areas Commun.*, vol. 27, no. 8, pp. 1379–1389, Oct. 2009.
[27] J. Qiao, L. X. Cai, X. Shen, and J. W. Mark, "STDMA-based scheduling algorithm for concurrent transmissions in directional millimeter wave networks," in *Proc. IEEE ICC*, Jun. 2012, pp. 5221–5225.
[28] A. Demers, S. Keshav, and S. Shenker, "Analysis and simulation of a fair queueing algorithm," in *Proc. Commun. Architect. Protocols*, 1989, pp. 1–12.
[29] A. Maltsev, "Channel models for 60 GHz WLAN systems," IEEE 802.11-09-0344-07ad, Mar. 2010.
[30] P. Dutta, V. Mhatre, D. Panigrahi, and R. Rastogi, "Joint routing and scheduling in multi-hop wireless networks with directional antennas," in *Proc. IEEE INFOCOM*, Mar. 2010, pp. 1–5.
[31] M. Puterman, *Markov Decision Processes: Discrete Stochastic Dynamic Programming*. Hoboken, NJ, USA: Wiley, 1994.
[32] D. P. Bertsekas, *Dynamic Programming and Optimal Control*, 3rd ed., vol. I/II. Belmont, MA, USA: Athena Scientific, 2011.

Jian Qiao received the B.E. degree from Beijing University of Posts and Telecommunications, China, in 2006 and the M.A.Sc. and the Ph.D. degrees from the Department of Electrical and Computer Engineering in the University of Waterloo, Canada, in 2010 and 2015, respectively. He is currently a Post-doc Fellow at the Department of Electrical and Computer Engineering, University of Waterloo, Canada. His research interests include millimeter wave communication, medium access control, resource management, 5G cellular networks, and mobile video streaming.

Xuemin (Sherman) Shen (M'97–SM'02–F'09) received the B.Sc. degree from Dalian Maritime University, China, in 1982 and the M.Sc. and Ph.D. degrees from Rutgers University, NJ, USA, in 1987 and 1990, respectively, all in electrical engineering. He is a Professor and University Research Chair, Department of Electrical and Computer Engineering, University of Waterloo, Canada. He was the Associate Chair for Graduate Studies from 2004 to 2008. His research focuses on resource management in interconnected wireless/wired networks, wireless network security, social networks, smart grid, and vehicular ad hoc and sensor networks. He is a co-author/editor of six books, and has published more than 600 papers and book chapters in wireless communications and networks, control and filtering. He is an elected member of IEEE ComSoc Board of Governor, and the Chair of Distinguished Lecturers Selection Committee. He served as the Technical Program Committee Chair/Co-Chair for IEEE Infocom'14, IEEE VTC'10 Fall, the Symposia Chair for IEEE ICC'10, the Tutorial Chair for IEEE VTC'11 Spring and IEEE ICC'08, the Technical Program Committee Chair for IEEE Globecom'07, the General Co-Chair for Chinacom'07 and QShine'06, the Chair for IEEE Communications Society Technical Committee on Wireless Communications, and P2P Communications and Networking. He also serves/served as the Editor-in-Chief for IEEE Network, Peer-to-Peer Networking and Application, and IET Communications; a Founding Area Editor for IEEE TRANSACTIONS ON WIRELESS COMMUNICATIONS; an Associate Editor for IEEE TRANSACTIONS ON VEHICULAR TECHNOLOGY, *Computer Networks*, and *ACM/Wireless Networks*, etc.; and the Guest Editor for IEEE JSAC, *IEEE Wireless Communications*, *IEEE Communications Magazine*, and *ACM Mobile Networks and Applications*, etc. He received the Excellent Graduate Supervision Award in 2006, and the Outstanding Performance Award in 2004, 2007 and 2010 from the University of Waterloo, the Premier's Research Excellence Award (PREA) in 2003 from the Province of Ontario, Canada, and the Distinguished Performance Award in 2002 and 2007 from the Faculty of Engineering, University of Waterloo. Dr. Shen is a registered Professional Engineer of Ontario, Canada, an IEEE Fellow, an Engineering Institute of Canada Fellow, a Canadian Academy of Engineering Fellow, and a Distinguished Lecturer of IEEE Vehicular Technology Society and Communications Society.

Jon W. Mark (M'62–SM'80–F'88–LF'03) received the Ph.D. degree in electrical engineering from McMaster University, in 1970. In September 1970, he joined the Department of Electrical and Computer Engineering, University of Waterloo, Waterloo, Ontario, where he is currently a Distinguished Professor Emeritus. He served as the Department Chairman during the period July 1984–June 1990. In 1996, he established the Center for Wireless Communications (CWC) at the University of Waterloo and is currently serving as its founding Director. He had been on sabbatical leave at the following places: IBM Thomas J. Watson Research Center, Yorktown Heights, NY, USA, as a Visiting Research Scientist (1976–77); AT&T Bell Laboratories, Murray Hill, NJ, USA, as a Resident Consultant (1982–83): Laboratoire MASI, Universit Pierre et Marie Curie, Paris France, as an Invited Professor (1990–91); and Department of Electrical Engineering, National University of Singapore, as a Visiting Professor (1994–95). He has previously worked in the areas of adaptive equalization, image and video coding, spread spectrum communications, computer communication networks, ATM switch design and traffic management. His current research interests are in broadband wireless communications, resource and mobility management, and cross domain interworking.

Prof. Mark is a Fellow of the Canadian Academy of Engineering. He is the recipient of the 2000 Canadian Award for Telecommunications Research and the 2000 Award of Merit of the Education Foundation of the Federation of Chinese Canadian Professionals. He was an editor of IEEE TRANSACTIONS ON COMMUNICATIONS (1983–1990), a member of the Inter-Society Steering Committee of the IEEE/ACM TRANSACTIONS ON NETWORKING (1992–2003), a member of the IEEE Communications Society Awards Committee (1995–1998), an editor of *Wireless Networks* (1993–2004), and an associate editor of *Telecommunication Systems* (1994–2004).

Lei Lei received the B.S. and Ph.D. degrees in telecommunications engineering from Beijing University of Posts and Telecommunications, China, in 2001 and 2006, respectively. From July 2006 to March 2008, she was a Postdoctoral Fellow at Computer Science Department, Tsinghua University, Beijing, China. She worked for the Wireless Communications Department, China Mobile Research Institute from April 2008 to August 2011. She has been an Associate Professor with the State Key Laboratory of Rail Traffic Control and Safety, Beijing Jiaotong University, since September 2011. Her current research interests include performance evaluation, quality-of-service and radio resource management in wireless communication networks.